

Charge-Transfer Complexation of C_{60} with Diphenyltetrathiafulvalene (DPTTF) Capped Gold Clusters

M. R. Resmi,* N. Sandhyarani,* R. Unnikrishnan,* Shuguang Ma,† and T. Pradeep*,†

*Department of Chemistry and Regional Sophisticated Instrumentation Centre, Indian Institute of Technology, Madras 600 036, India; and

†Department of Chemistry, Purdue University, West Lafayette, Indiana 47907

Received March 5, 1999; accepted May 28, 1999

4,4'-Diphenyltetrathiafulvalene (DPTTF) capped gold nanoparticles of 3- to 5-nm diameter have been prepared and their thermal stability has been investigated by variable temperature FT-IR spectroscopy. The DPTTF molecules at the cluster surface undergo charge-transfer complexation with C_{60} to form Au/DPTTF. C_{60} . Direct evidence of complexation is observed in the x-ray photoelectron and infrared spectra of the clusters. The orientational ordering transition of C_{60} in Au/DPTTF. C_{60} clusters occur at a higher temperature than pure C_{60} indicating increased resistance to orientational disorder due to charge transfer. Variable-temperature infrared spectroscopic studies yield complementary information. Both FT-IR and mass spectra show that some of the sites on the gold surface are occupied by the phase-transfer reagent used in the cluster preparation. © 1999 Academic Press

Key Words: self-assembled monolayers; gold nanoparticles; fullerenes; charge-transfer complex.

INTRODUCTION

Self-assembled monolayers (SAMs) of organic molecules, especially the monolayers of thiols prepared on planar gold surfaces (2D-SAMs) constitute an intensely investigated area of current science (1). Recently, monolayers self-assembled on small, well-defined metal clusters (3D SAMs) have received a great deal of attention because of their diverse physico-chemical properties and potential utility in wide range of technologies (2–4). The presence of higher monolayer concentration owing to the large surface area of the metal clusters as well as the fact they are soluble in various organic solvents make it possible to apply various analytical techniques like NMR, UV-VIS, and XRD on them which is difficult for the corresponding 2D monolayers (4).

The chemical derivatization of SAMs is an exciting area of research because of its potential application in building surfaces with novel properties. Detailed investigations of 2D-SAM derivatization are available in the literature (5). But studies on the reactivity of monolayers on 3D clusters are limited (6–7). A significant difference in reactivity is expected between SAMs on flat and 3D cluster surfaces for several

reasons. A major factor is the larger number of defect sites in 3D SAMs compared with the densely packed 2D monolayers. Another significant factor is the presence of a curved surface for the cluster which gives greater mobility for the terminal functional groups. Templeton *et al.* (7) reported a detailed study of the chemical reactivity of alkane thiolate monolayer protected gold clusters. They studied the reactivity of monolayers having various terminal functionalities and different chain lengths.

In the present work, we are concerned with the charge-transfer complexation chemistry of monolayers capped on gold clusters. Tetrathiafulvalene (TTF) and its derivatives are compounds well known as electron donors, which form charge-transfer complexes with electron acceptors like tetracyanoquinodimethane (8). The TTF derivatives like diphenyltetrathiafulvalene (DPTTF) and benzenedithiatetrathiafulvalene (BEDT-TTF) are known to form charge-transfer complexes with fullerenes and fullerene derivatives (9). C_{60} is a good electron acceptor due to the fact that it has low-lying unoccupied molecular orbitals. Therefore, we have chosen DPTTF as the capping agent for the gold nanoparticles and the charge-transfer complexation of the capped cluster with C_{60} has been investigated by various spectroscopic techniques.

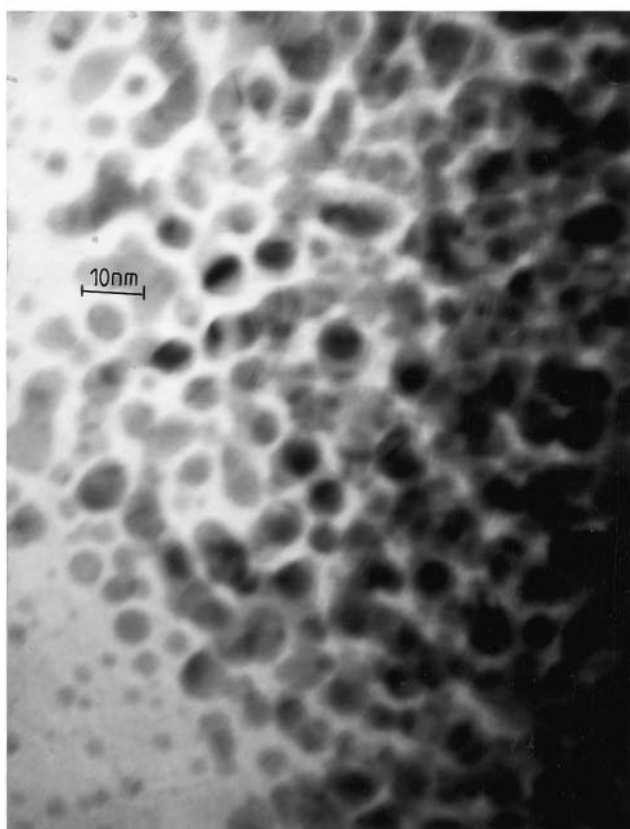
EXPERIMENT

A 61.8-ml toluene solution of tetra-*n*-octyl ammonium bromide (0.0358 M) was added to a vigorously stirred 30-ml 0.0288 M aqueous solution of $AuClO_4$. After 1 h of stirring, a 71.4 ml 0.015 M toluene solution of DPTTF was added and the resulting solution was stirred for 10 min. To this mixture, 24.7 ml aqueous solution of 0.3896 M sodium borohydride was added drop-wise over a period of about 1 h. The toluene phase develops a brown color due to the gold cluster formation. The solution was stirred overnight and the organic layer was separated from the aqueous phase. Half of the organic part was taken and concentrated to 10 ml, 100 ml of methanol was poured into this solution. The precipitated cluster was centrifuged, which could be redissolved and reprecipitated. It was then washed several times with methanol to remove the unreacted DPTTF and air dried. In the preparation of Au/

¹ To whom correspondence should be addressed. E-mail: pradeep@iitm.ernet.in.



(a)



(b)

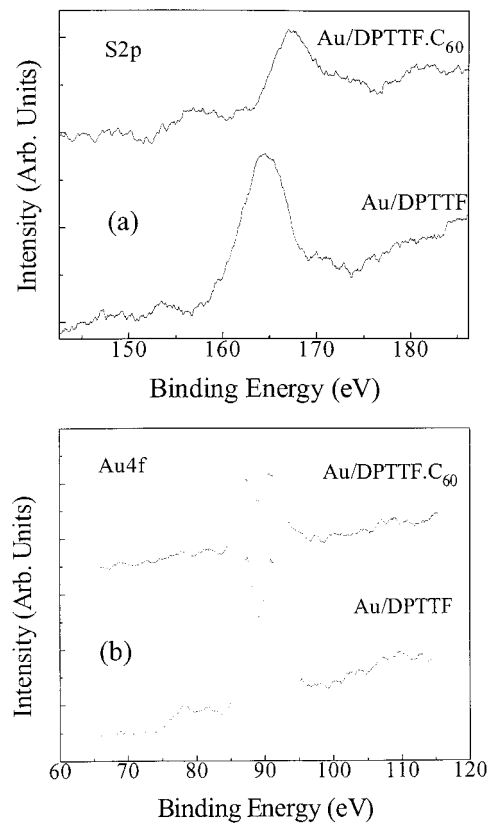
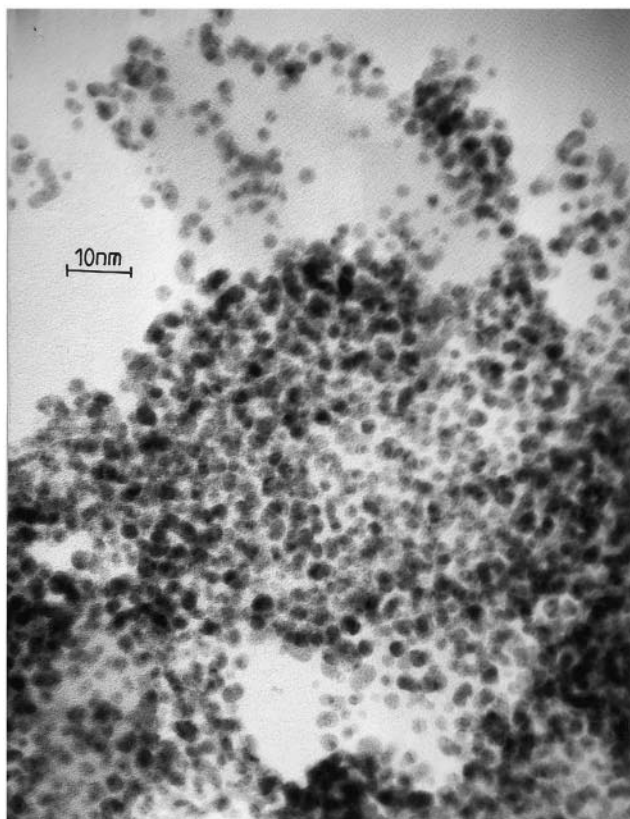


FIG. 2. X-ray photoelectron spectra (a) the S2p region and (b) Au4f region for the Au/DPTTF and the Au/DPTTF.C₆₀ clusters.

DPTTF.C₆₀, the other half of the organic part of the solution was taken and 20 ml 0.01 M C₆₀ solution in toluene was added. The solution was stirred overnight. It was then concentrated, 100 ml methanol was added, and the precipitated clusters were centrifuged, washed repeatedly with toluene to remove the unreacted DPTTF and C₆₀, and air dried. The C₆₀ complexed cluster was insoluble in most of the organic solvents.

Transmission electron micrographs were taken with a 200 keV JEOL JEM-2000EX microscope at Purdue University. X-ray diffraction patterns were measured with CuK α radiation. The samples were spread on antireflection glass slides to give uniform films. The films were wetted with acetone for adhesion and were blown dry before measurement. All samples were similarly prepared.

FT-IR studies were performed with a Bruker IFS66v FT-IR spectrometer and the temperature dependent measurements were done with a variable temperature (100–500 K) accessory fabricated in our laboratory. XPS measurements were conducted with a VG ESCALAB Mk II spectrometer with unmonochromatized MgK α radiation. Proton NMR measurements were done in CDCl₃ solutions of the samples with a 400

FIG. 1. The transmission electron micrographs of (a) the Au/DPTTF and (b) the Au/DPTTF.C₆₀ clusters.

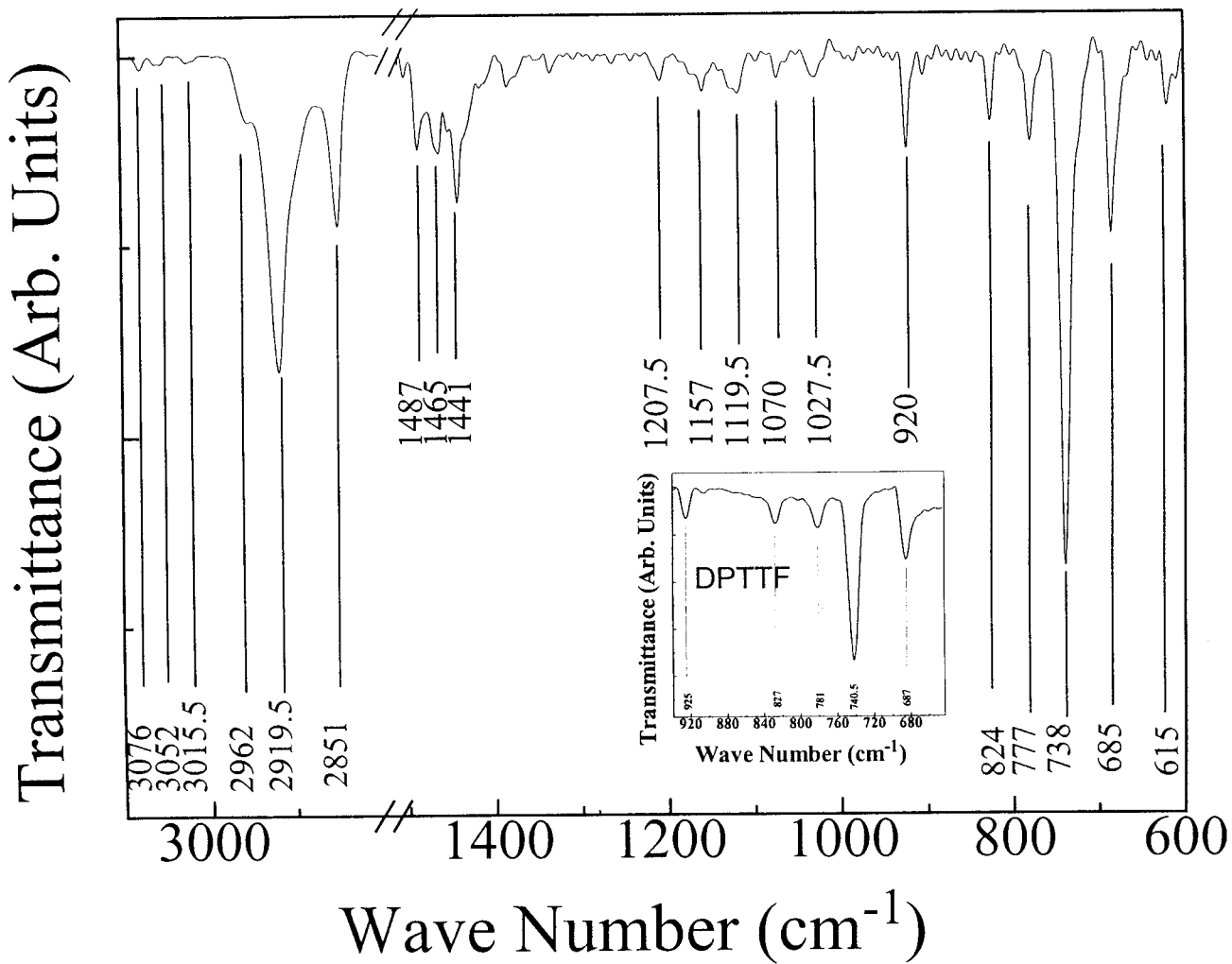


FIG. 3. The FT-IR spectrum of the Au/DPTTF clusters. The IR spectrum of solid DPTTF in the 900- to 650-cm⁻¹ region is shown in the inset.

MHz JEOL NMR spectrometer. The UV/VIS absorption measurements were taken using CDCl₃ solutions of the clusters with a VARIAN CARY-05 spectrophotometer.

Mass spectra were recorded with a TSQ700 triple quadrupole spectrometer. Samples were introduced as powders, coated on a filament, and heated up to 1473 K in a programmed fashion. Spectra acquired around the maximum in the total ion current were averaged and are reported as the mass spectra of the samples. Collision-induced dissociation spectra of several ions were done to make peak assignments. The ion of interest was mass selected ($\Delta m = 1$ amu) by the first quadrupole and was collided with Ar (0.4 mTorr) in the second quadrupole at 10 eV translational energy. The collision-induced dissociation spectra were measured with the third quadrupole.

RESULTS AND DISCUSSION

The detailed investigations toward the characterization of the Au/DPTTF and the Au/DPTTF.C₆₀ clusters were done by

various spectroscopic techniques like TEM, XRD, NMR, UV-VIS, FT-IR, and mass spectrometry. Variable temperature FT-IR measurements were carried out on the Au/DPTTF clusters for monitoring the decomposition pathway and to understand of the adsorption geometry and stability of the monolayers. Low-temperature FT-IR measurements were performed on the Au/DPTTF.C₆₀ clusters to study the effect of charge transfer from the DPTTF monolayer to the C₆₀ molecules on the orientational ordering transition of C₆₀.

Figures 1a and 1b are the TEM images for the Au/DPTTF and the Au/DPTTF.C₆₀ clusters, respectively. Both the images show that most of the particles have sizes less than 6 nm, confirming the nanocrystalline nature of the metal. For both the clusters, the diameters of the particles are in the 3- to 5-nm range. No agglomeration of the particles is seen which would have been observed had C₆₀ been in complexation with multiple clusters.

The powder X-ray diffraction patterns of the clusters are similar to those of the thiolate capped gold clusters (10). X-ray

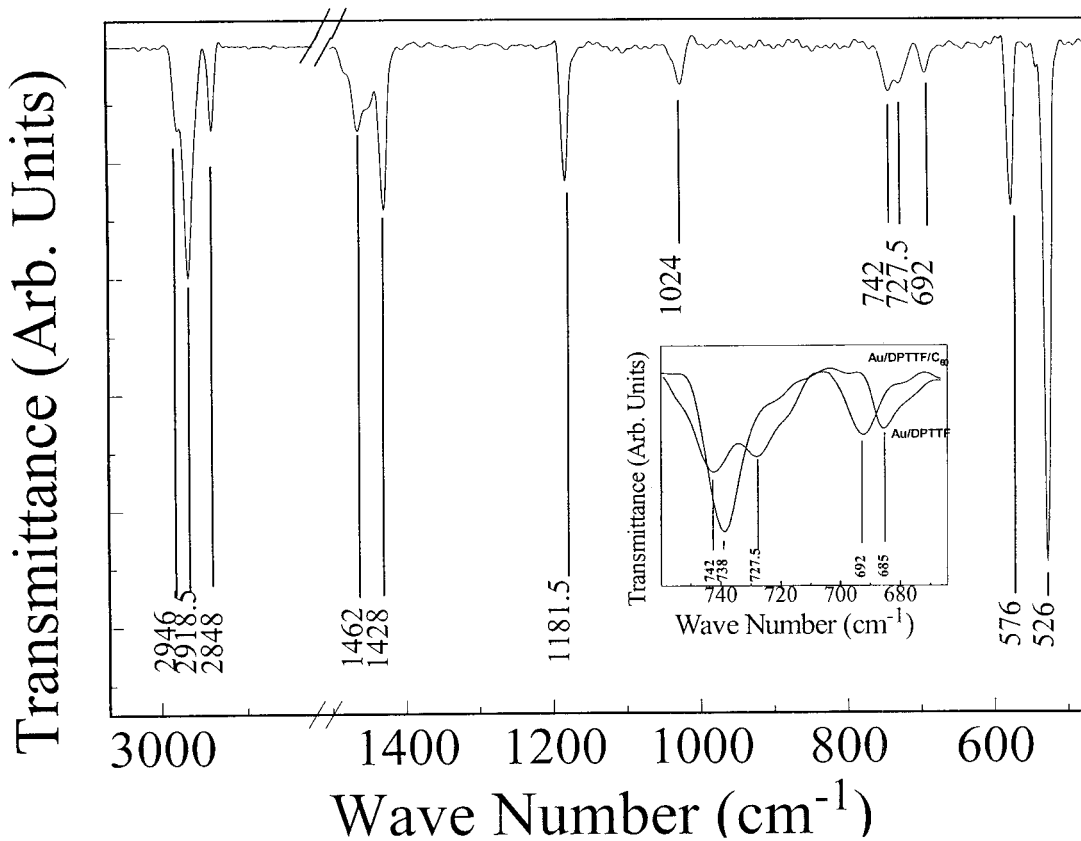


FIG. 4. The FT-IR spectrum of Au/DPTTF.C₆₀ clusters. The inset shows the shift in the C–S stretching region from the Au/DPTTF spectrum.

scattering is dominated by the metal core and contributions from the ligand is minimal. The diffraction patterns are almost identical to that of the bulk fcc gold except that they are broader due to the nanocrystalline nature of the particles. An analysis of the peak-widths on the basis of the Scherrer formula (11) gave cluster sizes which are in agreement with the TEM data. The powder diffraction profile of the two samples are identical indicating that the metal cluster dimension is unaffected upon complexation.

The S2p region of the x-ray photoelectron spectra of the samples is shown in Fig. 2a. For the Au/DPTTF cluster, the S2p peak occurs at 164.3 eV, whereas it appears at 167.2 eV for the Au/DPTTF.C₆₀ cluster. The presence of a peak around 164 eV is indicative of a covalently bound sulfur atom at the surface. This binding energy is slightly higher than the thiolate (R–S[–]) value normally found in alkane thiolate monolayers (162–164 eV) (12). The shift in the peak position to a higher value upon complexation is indicative of electron transfer to C₆₀ in accordance with the expectation. The fact that no additional sulfur structure is observed indicates that all the sulphur atoms of the DPTTF molecule are uniformly involved in electron transfer and complexation occurs with all of them. Figure 2b shows the Au4f region of the XPS spectra where the 4f_{7/2} and 4f_{5/2} bands are present at 88 and 91 eV, respectively, for both the Au/DPTTF and Au/DPTTF.C₆₀ clusters. We did not

see any shift in the position or asymmetry in the peak shape, which suggests that the majority of gold atoms are in their zero oxidation state. This is in accordance with the data of alkane-thiol capped clusters as well (13).

In the FT-IR spectrum of the DPTTF clusters (Fig. 3), the C–S stretching vibrations and the pentagonal ring deformation modes of the DPTTF molecules occur in the 900–650 cm^{–1} region, which is almost similar to the pristine DPTTF spectrum (shown in the inset of Fig. 3) except for a slight downward shift in peak positions for the cluster due to adsorption. The spectral assignments are based on the detailed vibrational analysis of TTF present in the literature (14). The bands at 685 and 738 cm^{–1} can be assigned to the CS stretching vibrations and the bands at 920, 824, and 777 cm^{–1} have contributions from ring SCC bending and external CCS bending modes. In the high-frequency region, the bands at 3076, 3052, and 3015.5 cm^{–1} correspond to the CH stretching vibrations of the benzene rings as well as the stretching vibrations of CH groups of the TTF moiety. In spite of thorough washing of the samples with toluene, the FT-IR spectrum shows peaks corresponding to the phase transfer reagent, tetraoctylammonium bromide. This may be because the Au–S bonds formed by the DPTTF could be weaker compared to the other monolayers such as alkane thiols. Thus in the high-frequency region of the FT-IR spectrum, the bands at 2962, 2919.5, and 2851 cm^{–1} can be attrib-

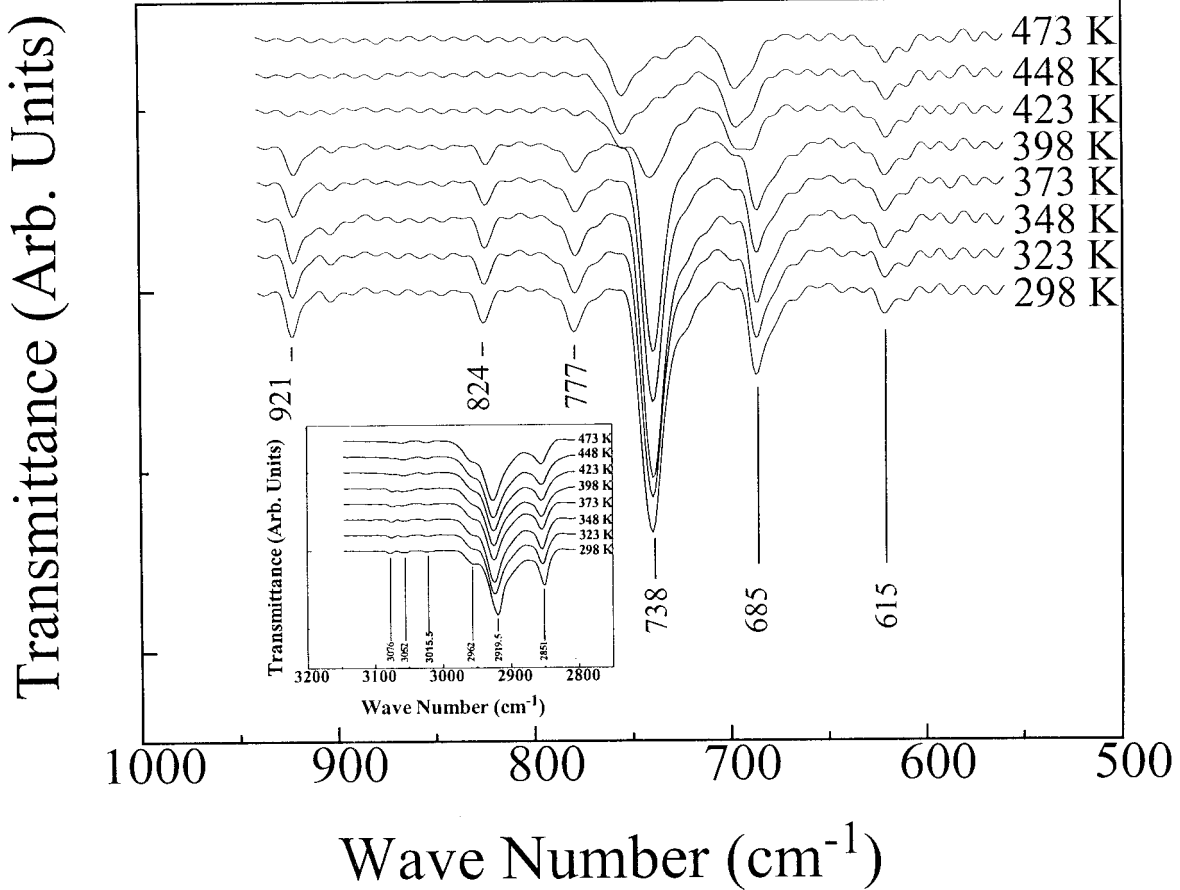


FIG. 5. The variable temperature FT-IR spectra of the Au/DPTTF clusters in the 900- to 650-cm⁻¹ region. The high-frequency region is shown in the inset. Temperatures are marked.

uted to the symmetric and antisymmetric C-H stretching vibrations of the methyl and methylene groups, and the bands at 1207.5, 1157, 1119.5, 1070, and 1027.5 cm⁻¹ can be assigned to the CH₂ wagging and rocking modes of the octyl chains of the phase transfer reagent. The corresponding methylene scissoring modes appear at 1487, 1465, and 1441 cm⁻¹.

In the FT-IR spectrum of Au/DPTTF.C₆₀ clusters (Fig. 4), the four peaks corresponding to the C₆₀ vibrations are observed at 1428, 1181.5, 576, and 526 cm⁻¹. The C-S stretching band at 685 cm⁻¹ is showing an 8-cm⁻¹ shift toward the higher frequency side (inset of Fig. 4) and the band at 738 cm⁻¹ is getting split into two peaks at 742 and 727.5 cm⁻¹.

In complexes with extensive charge-transfer (CT) like C₆₀Br₈.TTF₈ (9c), a remarkable decrease in the frequency of the vibrational bands of the fullerene is observed corresponding to multi-electron transfer. But in most of the CT complexes, where there is only partial electron transfer, the downshift of the vibrational bands is by a value less than 4 cm⁻¹ as in the case of C₆₀.HMTTF complex (9d). In the FT-IR spectrum of Au/DPTTF.C₆₀ clusters, the C₆₀ bands at 527 and 1429 cm⁻¹ are showing a 1-cm⁻¹ downshift with respect to the C₆₀ spectrum. The increase in the frequency of the TTF modes and the corresponding frequency decrease for the C₆₀ modes,

although small, are indicative of a weak charge-transfer interaction.

In the spectrum, the peaks in the 3000- to 2800-cm⁻¹ region can be attributed to the vibrations of the hydrocarbon chain of the phase transfer reagent impurity. The methylene scissoring mode appears at 1462 cm⁻¹. The wagging and rocking progression bands are showing substantial difference when compared to the Au/DPTTF spectrum. This difference coupled with the changes in the aliphatic CH stretching region is indicative of changes in the organization of the alkyl chains.

The variable temperature FT-IR spectra of the Au/DPTTF clusters (Fig. 5) show that the DPTTF monolayer is quite stable up to 398 K and there is essentially no change in the 600- to 900-cm⁻¹ region up to this temperature except an overall decrease in intensity due to the slow desorption of the monolayer at higher temperatures. From 423 K onward, a change in the spectral profile is observed in this region. The bands at 738 and 685 cm⁻¹ are shifted to 749 and 700 cm⁻¹, respectively, whereas the bands at 921, 824, and 777 cm⁻¹ are disappearing. A corresponding sudden intensity decrease for the peak at 3076 cm⁻¹ corresponding to the aromatic CH stretching vibration is also observed. The changes can be attributed to the change in the orientation of the fulvalene moiety along with subsequent

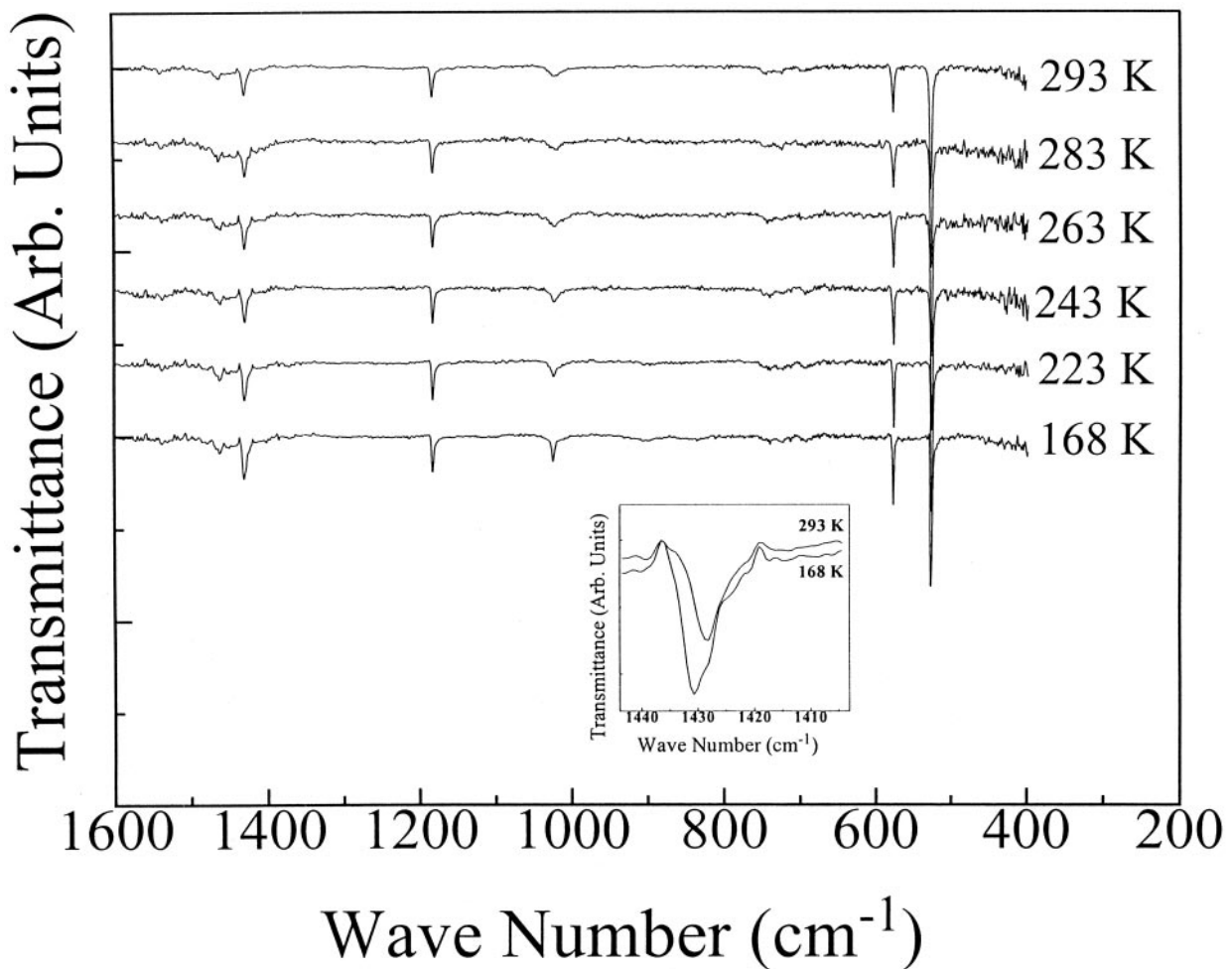


FIG. 6. The variable temperature FT-IR spectra of the $\text{Au}/\text{DPTTF} \cdot \text{C}_{60}$ clusters. The inset shows the change for the pentagonal pinch mode before and after the orientational ordering transition. The temperatures are marked.

changes in the phenyl ring orientations without the breakage of the $\text{Au}-\text{S}$ bonding at 423 K. The spectra at 423 and 448 K show multiple geometries at the surface whereas in the high-frequency region, the C–H stretching vibrations at 2919.5 and 2851 cm^{-1} show a 2-cm^{-1} shift to higher frequency at 323 K, indicating the melting of the alkyl chains of the phase transfer reagent.

One of the possible methods of observing the charge transfer of the DPTTF monolayer to C_{60} is the study of the orientational ordering transition of C_{60} . Fullerenes and their highly symmetrical derivatives are known to undergo first-order phase transitions which are orientational in nature involving essentially the freezing of the free rotations of the molecules (15, 16). The orientational ordering transition of C_{60} occurs around 249 K. Any form of charge transfer to the fullerene cage or bonding which can hinder the free rotations to some extent will increase the temperature for rotational freezing. We have studied the orientational ordering transition of C_{60} in the $\text{Au}/\text{DPTTF} \cdot \text{C}_{60}$ clusters by differential scanning calorimetry and variable temperature FT-IR spectroscopy.

In the FT-IR spectrum of C_{60} , the pentagonal pinch mode appearing at 1429 cm^{-1} is the most sensitive band for the orientational ordering transition (16). For the $\text{Au}/\text{DPTTF} \cdot \text{C}_{60}$ cluster, the pentagonal pinch mode of C_{60} appears at 1428 cm^{-1} in the room-temperature IR spectrum. In the variable temperature FT-IR studies (Fig. 6) this band shows a 3-cm^{-1} shift to higher frequency along with an intensity increase around 263 K (shown in the inset of Fig. 6). The extent of shift and the narrowing of the band profile is comparable to that of pure C_{60} .

The mass spectra for the Au/DPTTF and $\text{Au}/\text{DPTTF} \cdot \text{C}_{60}$ clusters, respectively, are shown in Figs. 7a and 7b. In the mass spectrum of Au/DPTTF cluster (Fig. 7a), a peak at m/z 356 is due to the molecular ion $\text{C}_{18}\text{H}_{12}\text{S}_4^+$ of DPTTF and the peak at m/z 102 can be assigned to the $\text{C}_3\text{H}_2\text{S}_2^+$ fragment from the TTF moiety. The peaks at m/z 466, 353, 254, and 156 can be attributed to the phase-transfer reagent. The former is due to the molecular ion of the phase transfer reagent $(\text{C}_8\text{H}_{17})_4\text{N}^+$ and latter are its fragments. In the mass spectrum of $\text{Au}/\text{DPTTF} \cdot \text{C}_{60}$ (Fig. 7b), the peaks at m/z 720 and 360 are due to C_{60}^+ and C_{60}^{2+} which dominate the mass spectrum. The difference in the

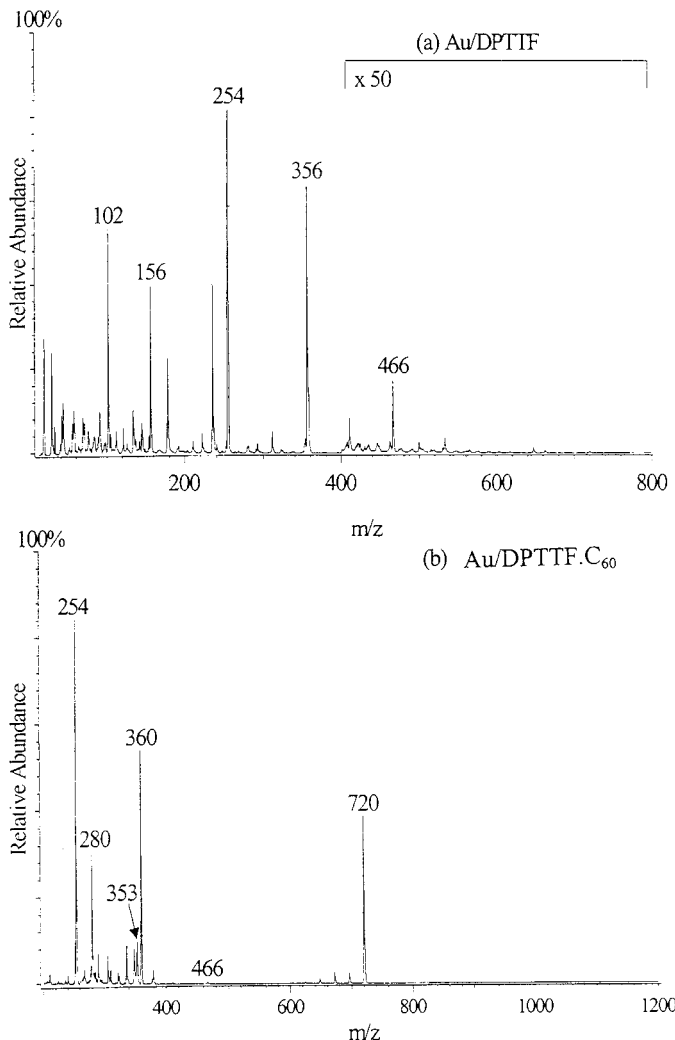


FIG. 7. Mass spectra of (a) the Au/DPTTF and (b) the Au/DPTTF.C₆₀ clusters. Mass numbers of the peaks of importance are labeled.

intensities of the C₆₀ and DPTTF peaks are presumably due to the difference in their ionization efficiencies. The peak at *m/z* 280 is the C₁₂H₈S₄⁺ fragment arising due to a phenyl loss from the DPTTF molecular ion. Here also, the peaks at *m/z* 466, 353, 254, and 156 can be attributed to the (C₈H₁₇)₄N⁺ and its fragments from the phase-transfer reagent.

Thus, derivatization of gold nanoparticle surfaces by means of charge transfer can be achieved by selecting monolayers of suitable donor molecules like tetrathiafulvalenes and acceptors like C₆₀, expanding the scope of surface modification of 3D-SAMs. The present work illustrates the possibility of putting materials with novel properties like fullerenes on top of a monolayer surface. The absence of dense packing unlike in the self-assembly on flat surfaces gives considerable flexibility for the donor molecules which is an important factor to have an effective charge transfer with the spherical fullerene molecules. From the variable-temperature FT-IR and DSC studies, it can be concluded that even though the charge transfer from the DPTTF monolayer is not strong enough to completely

eliminate the dynamical disorder of fullerenes, it does have an effect on the temperature of the orientational ordering. It is to be noted that the DPTTF molecules appear to lie flat on the surface since all the sulfur atoms seem to be involved in bonding. This means that C₆₀ molecules must approach very close to the surface to allow complex formation. Thus, the long alkyl chains of the phase-transfer reagent molecules, which are shown to be present on the surface, are sufficiently flexible to allow the penetration of fullerenes.

ACKNOWLEDGMENTS

T.P. thanks the Department of Science and Technology, Government of India for supporting his research programme on monolayers. M.R.R. and N.S. thank the Council of Scientific and Industrial Research for Research Fellowships. Part of this research was carried out at Purdue University when T.P. was a Senior Fulbright Fellow in the laboratory of Prof. Graham Cooks. Dr. Said Mansour is thanked for the transmission electron micrographs.

REFERENCES

- (a) See for example, Bain, C. D., Troughton, E. B., Tao, Y. T., Evall, J., Whitesides, G. M., and Nuzzo, R. G., *J. Am. Chem. Soc.* **111**, 321 (1989). (b) Finkele, H. O., Avery, S., and Lynch, M., *Langmuir* **3**, 409 (1987). (c) Bain, C. D., Davies, P. B., Ong, T. H., Ward, R. N., and Brown, M. A., *Langmuir* **7**, 1563 (1991). (d) Whitesides, G. M., and Laibinis, P. E., *Langmuir* **6**, 87 (1990). (e) Allara, D. L., and Nuzzo, R. G., *Langmuir* **1**, 52 (1985). (f) Chidsey, C. E. D., Liu, G. Y., Rountree, P., and Scoles, G., *J. Chem. Phys.* **91**, 4421 (1989). (g) Tao, Y.-T., Wu, C.-C., Eu, J.-Y., and Lin, W.-L., *Langmuir* **13**, 4018 (1997); Porter, M. D., Bright, T. B., Allara, D. L., and Chidsey, C. E. D., *J. Am. Chem. Soc.* **109**, 3559 (1987); Nuzzo, R. G., Dubois, L. H., and Allara, D. L., *J. Am. Chem. Soc.* **112**, 558 (1990); Nuzzo, R. G., Fusco, F. A., and Allara, D. L., *J. Am. Chem. Soc.* **109**, 2358 (1987).
- Hostettler, M. J., and Murray, R. W., *Curr. Op. Colloid Interface Surf.* **2**, 42 (1997).
- (a) Wang, Y., and Herron, N., *J. Phys. Chem.* **95**, 525 (1991). (b) Schmid, G., *Chem. Rev.* **92**, 1709 (1992). (c) Hoffman, A. J., Mills, G., Yee, H., and Hoffman, M. R., *J. Phys. Chem.* **96**, 5546 (1992). (d) Green, S. J., Stokes, J. J., Hostettler, M. J., Pietron, J., and Murray, R. W., *J. Phys. Chem.* **101**, 2663 (1997). (e) Storhoff, J. J., Elghanian, R., Mucic, C., Mirkin, C. A., and Letsinger, R. L., *J. Am. Chem. Soc.* **120**, 1959 (1998). (f) Mandler, D., and Turyan, I., *Electroanalysis* **8**, 207 (1996).
- Terrell, R. H., Postlethwaite, T. A., Chen, C.-H., Poon, C.-D., Terzis, A., Chen, A., Hutchison, J. E., Clark, M. R., Wignall, G., Londono, J. D., Superfine, R., Falvo, M., Johnson, C. S., Jr., Samulski, E. T., and Murray, R. W., *J. Am. Chem. Soc.* **117**, 12537 (1995).
- Ulman, A., "An Introduction to Ultrathin Organic Films: From Langmuir Blodgett to Self Assembly." Academic Press, New York, 1991; Ulman, A., *Chem. Rev.* **96**, 1533 (1996).
- Shi, J., Gider, S., Babcock, K., and Awschalom, D. D., *Science* **271**, 937 (1996).
- Templeton, A. C., Hostettler, M. J., Kraft, C. T., and Murray, R. W., *J. Am. Chem. Soc.* **120**, 1906 (1998).
- Wudl, F., Smith, G. M., and Hufnagel, E. J., *J. Chem. Soc., Chem. Commun.*, 1453 (1953); Coleman, L. B., Cohen, M. J., Sandman, D. J., Yamagoshio, M. J., Garito, A. F., and Heeger, A. J., *Solid State Commun.* **12**, 1125 (1973).
- (a) Yang, Y., *J. Phys. Chem.* **96**, 764 (1992); (b) Izuoka, A., Tachikawa, T., Sugawara, T., Saito, Y., and Shinohara, H., *Chem. Lett.*, 1049 (1992); Izuoka, A., Tachikawa, T., Sugawara, T., Suzuki, Y., Konno, M., Saito, Y., and Shinohara, H., *J. Chem. Soc. Chem. Commun.*, 1473 (1992); (c) Rao, C. N. R., Govindraj, A., Sumathy, R., and Sood, A. K., *Mol. Phys.* **88**,

11 (1996); (d) Pradeep, T., Singh, K. K., Sinha, A. P. B., and Morris, D. E., *J. Chem. Soc. Chem. Commun.*, 1747 (1992).

10. Leff, D. V., Brandt, L., and Heath, J. R. *Langmuir* **12**, 4723 (1996); Brust, M., Fink, J., Bethell, D., Schiffrin, D. J., and Kiely, C., *J. Chem. Soc. Chem. Commun.*, 1655 (1995).

11. West, A. R., "Solid State Chemistry and Its Applications." Wiley, New York, 1987.

12. Brust, M., Walker, M., Bethell, D., Schiffrin, D. J., and Whyman, R. *J. Chem. Soc. Chem. Commun.*, 801b (1994).

13. Johnson, S. R., Evans, S. D., Mahon, S. W., and Ulman, A., *Langmuir* **13**, 511 (1997).

14. Bozio, R., Girlando, A., and Pecile, D., *Chem. Phys Lett.* **52**, 503 (1977); Bozio, R., Zanon, I., Girlando, A., and Pecile, D., *J. Chem. Phys.* **71**, 2282 (1979); Seidle, A. R., Candela, G. A., Finnegan, T. F., Van Duyne, R. P., Cape, T., Kokoszka, G. F., Woyciejes, P. M., and Hashmall, J. A., *Inorg. Chem.* **20**, 2635 (1981).

15. Heiney, A., Fisher, J. E., McGhie, A. R., Romanow, W. J., Denenstein, A. M., McCauley Jr., J. P., Smith III, A. B., and Cox, D. E., *Phys. Rev. Lett.* **67**, 1467 (1991); van Loosdrecht, P. H. M., van Bentum, P. J. M., and Meijer, G., *Phys. Rev. Lett.* **68**, 1176 (1992); Michel, K. H., *J. Chem. Phys.* **97**, 5155 (1992).

16. Resmi, M. R., George, L., Singh, S., Shankar, U., and Pradeep, T., *J. Mol. Struct.* **435**, 11 (1997); Resmi, M. R., Smitha, K., Arunagiri, T. N., and Pradeep, T., *Full. Sci. Technol.* **7**, 123 (1999).